

# A METROLOGICAL ANALYSIS OF THE IGPS SYSTEM FOCUSING ON ITS MAIN SOURCES OF UNCERTAINTIES

*Bolívar Landeta*<sup>1</sup>, *Ricardo Sutério*<sup>2</sup>, *Luís Gonzaga Trabasso*<sup>3</sup>

<sup>1</sup> Instituto Tecnológico de Aeronáutica - ITA, São José dos Campos, Brasil, bolivar@ita.br

<sup>2</sup> Instituto Nacional de Pesquisas Espaciais – INPE, São José dos Campos, Brasil, suterio@lit.inpe.br

<sup>3</sup> Instituto Tecnológico de Aeronáutica - ITA, São José dos Campos, Brasil, gonzaga@ita.br

**Abstract:** The iGPS is a metrological system designed principally for large volumes. Thus, this system possesses different uncertainty sources related to measuring procedure, the very measuring system, environmental conditions, among others. Through evaluation experiments, the main sources related to measurement strategy were identified and the iGPS datasheet uncertainty was reached.

**Key words:** iGPS, uncertainty, measuring process, measurand.

## 1. INTRODUCTION

The iGPS (indoor Global Positioning System) system is relatively new one in the global metrological sector. This system with accuracy up to tenths of a millimeter is designed to large scale metrology. There are a few iGPS published works, as to control and track a non-holonomic trajectory of a mobile robot [1]. Other work carried out iGPS accuracy measures in terms of the equipment distribution on a particular work area [2]. Using another optical measuring system, the Laser Tracker, both systems tolerances were compared in large volumes related to aerospace parts and subassemblies [3]. Additionally, another iGPS work related optical measurement techniques of mobile metrology in large volumes, explaining briefly its operating principle [4]. Up to now, even fewer iGPS works related to its uncertainty measure have been published. So, the works of Muelaner et al [5] and ARCSECOND [6], that shows uncertainty values obtained experimentally from a specific iGPS component, serve like reference to the present work.

The present work presents an analysis of the iGPS metrological reliability focusing on its main sources of uncertainty through evaluation experiments results.

## 2. IGPS SYSTEM

The iGPS is composed of transmitters emitting laser signal that is captured by a set of sensors located within a volume work. This system uses the physical principle of triangulation that is also used in the current global positioning system. Thus, the iGPS transmitters act like satellites and the iGPS sensors represent the desired location points on the earth surface [7]. 3D information is necessary to set a location point in the space; this is attained using spherical coordinates through sensors elevation and azimuth angles in relation to a spinning transmitter head. Each transmitter head rotates at a specific frequency and emits two laser beams, as well as, a stroboscopic infrared signal

that is captured by sensors located in the mini-vector bars or in the iProbe [8]. Fig. 1 shows the iGPS elements.

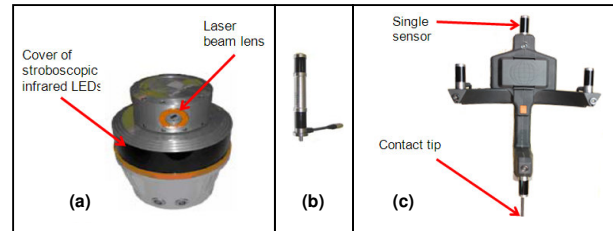


Fig. 1. iGPS main elements: (a) Transmitter, (b) Mini-Vector Bar, (c) iProbe. Source: METRIS [9].

Figure 2 explains the azimuth and elevation angles interaction. Because the inclination angle of the two laser beams is known, the angular value is converted to azimuth and elevation angles. So, the time difference between the passage of laser beams 1 and 2 (see Fig. 2) defines the elevation angle ( $\theta$ ) due to beams inclination. The azimuth angle ( $\phi$ ) is defined as the difference between the periodic reference pulse and the mid-point in the passage of two laser beams. Thus, the two angles of elevation and azimuth define the radius of the transmitter to the sensor.

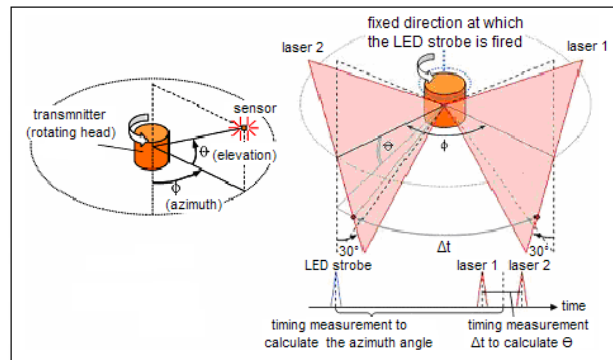


Fig. 2. Azimuth and elevation angles. Source: Maisano et al [10].

Because a sensor position cannot be known with only one transmitter, at least, another transmitter is necessary to use the triangulation principle. Whenever more transmitters are used, the system accuracy increases (METRIS [9]).

## 3. IGPS METROLOGICAL ANALYSIS

### 3.1. Error Sources

The iGPS possesses different error or uncertainty sources, related to measuring procedure, the very measuring system,

environmental conditions, and measurand / operator definitions. Fig. 3 shows all error sources considered in the present analysis.

In the analysis of error propagation were used only sources of uncertainty that could be quantified based on manufacturer data, as well as, on iGPS experiments carried out and other works related to these topic ([5] and [6]). Other sources, such as vibrations and air flows (environmental conditions) are only mentioned and quantified due lack of data.

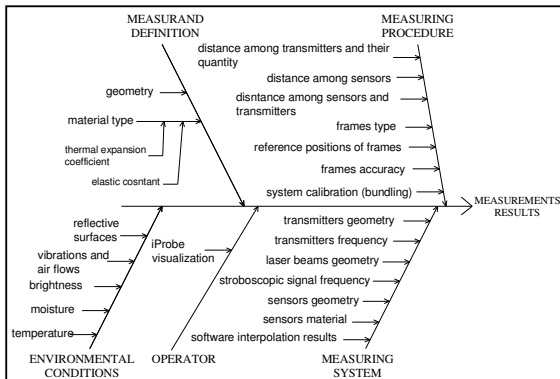


Fig. 3. iGPS error sources. Source: Landeta [11].

### 3.2. iGPS uncertainties considered

In this work the terminology adopted is that of the International Vocabulary of Metrology: basic and general concepts and associated terms (VIM - 2005) (INMETRO, 2005) [12] and the procedure for uncertainties calculation based on the 3rd. Brazilian edition of the Guide to the Expression of Uncertainty in Measurement (ISO-GUM) (INMETRO, 2003) [13]. Additionally, indications about measurement uncertainties determination related to the CMM (Coordinate Measure Machine) on ISO / DTS 15330-3 (ISO, 2000) [14] were considered as well.

Considering the elements that make up the system iGPS and others involved in the measurement process, the uncertainty sources were categorized and identified as follows:

#### 3.2.1 Transmitters

Laser beams geometry.

$X_1$  = azimuth angle,

$X_2$  = elevation angle,

$X_3$  = laser beam symmetry,

System calibration

$X_4$  = transmitter average error,

Noises / Vibrations

$X_5$  = transmitter head oscillation because of the rotation axis precession (longitudinal axis z),

$X_6$  = rotation noise by the imperfections of axis - bearings interface.

#### 3.2.2 Sensors

Materials

$X_7$  = geometry / material between two sensors of the mini-

vector bar and the iProbe,

$X_8$  = geometry of the sensors cylindrical surface that is composed of flat surfaces,

Amplifier

$X_9$  = amplifier pulse distortion,

Sampling clock

$X_{10}$  = sampling error in the analog to digital conversion,

System calibration

$X_{11}$  = error of virtual local coordinate system used as a reference system,

$X_{12}$  = error of local coordinate system of the mini-vector bar,

$X_{13}$  = iProbe calibration,

Positioning

$X_{14}$  = laser beam reflection between the vector mini-bars because of the distance between them.

#### 3.2.3 Scale bar

Material

$X_{15}$  = geometry / material of the scale bar.

#### 3.2.4 Sample test

Measurements

$X_{16}$  = standard deviation of distance measurements of a mini-vector bar,

Material

$X_{17}$  = geometry / material of the sample test.

#### 3.2.5 Environmental conditions

$X_{18}$  = temperature / moisture of work area,

$X_{19}$  = vibrations and air flows during measurements,

$X_{20}$  = brightness / reflective surface of work area.

Because most of the magnitudes indicated depend on the positioning of measuring system elements and the calibration mode of the work area, the approach adopted for the uncertainty analysis is in the best measurement condition obtained in one of the evaluation experiments carried out by Landeta and Sutério [8]. This experiment measures the distances ( $D_0$  and  $D_I$ ) of each one of the two mini-vector bars considering a local coordinate system that in theory its origin matches with  $D_0$ . The layout of this experiment as well as its configuration is depicted in the Fig. 4.

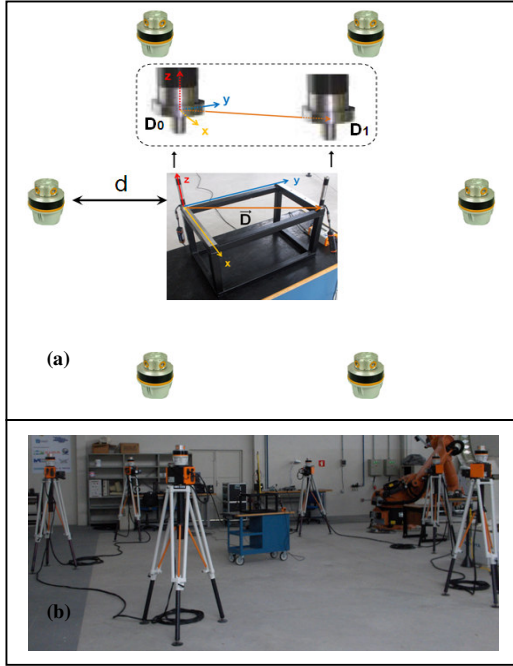


Fig. 4. Experimental configuration: (a) Transmitter and sensors layout position around the sample test. (b) Transmitters position around sensors located on the sample test. Source: Landeta and Sutério [8].

The best measurement condition posses six transmitters that are located symmetrically around the sample test, the distance  $D_1$  measured only with mini-vector bars  $d = 7$  m (transmitter-sensor distance) and an average of three measurements of  $D_1 = 598$  mm. The Fig. 5 shows this best measurement condition with the smallest error ( $\Delta D_1$ ) that represents the distance difference between the iGPS measurement and the nominal one measured with a coordinate measuring machine (brand: Zeiss, model: MD-049/09, measure uncertainty:  $\pm 14 \mu\text{m}$  with 95% confidence level.) [8]

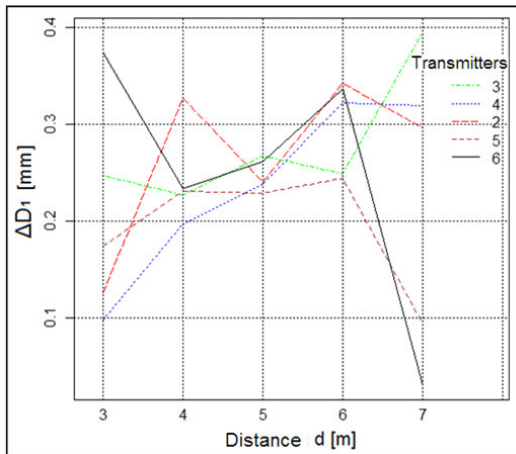


Fig. 5. Transmitter quantity interaction. Source: Landeta and Sutério [8].

### 3.3 Considerations of uncertainty values

In the experimental work carried out by Muelaner et al [5] on the uncertainties about angles measuring of the iGPS

transmitters, they were found angular uncertainties related to the transmitter concentricity with its longitudinal rotation axis z, sensor instabilities, parallelism and azimuth angle because of refractive changes in the air.

A combination of these uncertainties for a confidence level of 95% results in an uncertainty of  $\pm 0.5''$  in the azimuth angle. Although Muelaner et al [5] suggest that the elevation angle uncertainty must be less than this value, for the analysis of this work is being considered the same value of azimuth angle uncertainty ( $\pm 0.5''$ ).

The geometric equations of the angles used by Muelaner et al. [5] are the same used in this study to determine the sensor errors positioning errors and it in Eq. (1):

$$E\theta_r = \tan^{-1}\left(\frac{E_r}{r}\right) \quad (1)$$

where:

- $E\theta_r$  = Single angular measurement error due to instability of sensor support,
- $E_r$  = Sensor error positioning,
- $r$  = Radial distance between transmitter and sensor.

For this work, a distance  $r = 7$  m was considered. Therefore, the sensor positioning error  $E_r$  is approximately equal to  $\pm 0.017$  mm that represents the uncertainty values of elevation ( $X_1$ ) and azimuth angles ( $X_2$ ).

According to ARC SECOND [6], the uncertainty contributions related to the iGPS transmitters are laser beam symmetry ( $X_3$ ) that posses an angular value of  $1''$ , the rotation axis precession ( $X_5$ ) equal to  $0.5''$  and the rotation noise by axes – bearings imperfections ( $X_6$ ) is also  $0.5''$ . The uncertainties correspond to sensors are the amplifier pulse distortion ( $X_9$ ) equal to  $2.5''$  and the sampling error in the analog to digital conversion ( $X_{10}$ ) equal to  $0.82''$ .

The last angular errors are converted to linear errors using the relation showed in the Eq. (2) which  $E_L$  results are similar to those used in the Eq. (1) for  $E_r$ .

$$E_L = \frac{A \cdot \pi \cdot r \cdot 1000}{3600 \cdot 180} \quad (2)$$

where:

- $E_L$  = Linear error [mm],
- $A$  = Angular error [°],
- $r$  = Radial distance between transmitter and sensor [m].

Furthermore, according to the same work of ARC SECOND [6], the flat surfaces that form the cylindrical surface of sensors ( $X_8$ ) generate an uncertainty of  $\pm 0.03$  mm.

Other magnitudes such as  $X_4$ ,  $X_{11}$ ,  $X_{12}$ ,  $X_{13}$  and  $X_{16}$  are represented by values obtained during the iGPS experimental evaluation and pre-established conditions. Therefore, the adopted values are:

The average transmitter error ( $X_4$ ) equal to  $0.122$  mm is showed in the Fig. 6.

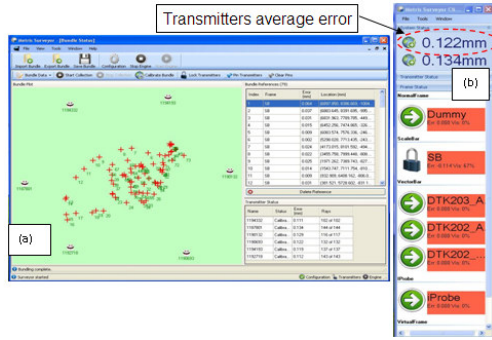


Fig. 6. Screen shots of the iGPS software for 6 transmitters and a distance  $d = 7m$ . Source: Landeta [11].

The error of the virtual local coordinate system ( $X_{11}$ ) equal to 0.037 mm is represented in the Fig. 7.

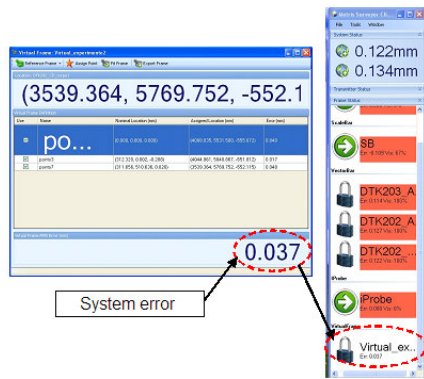


Fig. 7. Screen shots of the iGPS software of a virtual coordinate system for 6 transmitters and a distance  $d = 7m$ . Source: Landeta [11].

The error of local coordinate system of the mini-vector ( $X_{12}$ ) (0.132 mm) uses an average value of the local coordinate systems errors (three measurements for six transmitters and  $d = 7m$ ) [11].

The error related to standard deviation of three measurements of  $D_1$  distance equal to 0,012 mm (six transmitters and  $d = 7m$ ) [11].

The iProbe calibration error ( $X_{13}$ ) is not considered in the present analysis because after many attempts, it was not possible to get a value lower than 0.314 mm [11].

Using an experiment carried out by Landeta [11] where it was determined the influence of the distance between mini-vector bars with a fixed quantity of transmitters; the uncertainty related to the laser beam reflection between two vector mini-bars ( $X_{14}$ ) is equal to 0,447 mm. This value ( $\Delta D$ ) was obtained from the linear regression model of the data curve depicted in the Fig. 8 for a distance  $D = 598.229$  mm (nominal module of  $D_1$  measured with the same coordinate measuring machine previously refereed).

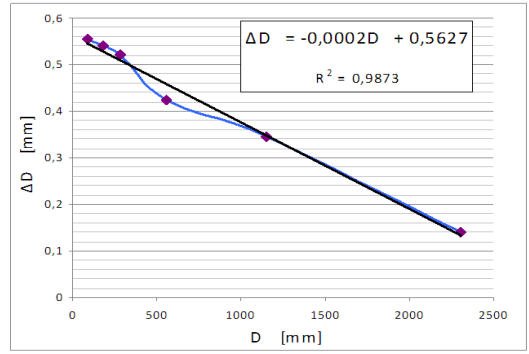


Fig. 8. Distance between mini-vector bars  $D$  vs. Measures difference  $\Delta D$ . Source: Landeta [11].

The mini-vector bar material, between its two sensors, is basically composed of stainless steel 14-7 with a low thermal expansion coefficient of  $2 \mu m/^\circ C$ . Thus, according to the mini-vector bar length, its geometry / material error ( $X_7$ ) is not considered because of its low value. A similar case happens with the scale bar material ( $X_{15}$ ) since it is of carbon composite type.

The sample test material is built of structural steel with  $0,000012 \text{ }^\circ C^{-1}$  thermal expansion coefficient. Thereby, using the Eq. (3) and considering an average temperature of  $25 \text{ }^\circ C$  during the measurements, the length change that represents its respective contribution of uncertainty is around 0.036 mm ( $X_{17}$ ).

$$\Delta L = \alpha \cdot L_i \cdot \Delta T \quad (3)$$

where:

- $\Delta L$  = Linear thermal expansion of  $D_1$  distance [mm],
- $\alpha$  = Linear thermal expansion coefficient ( $0,000012 \text{ }^\circ C^{-1}$ ),
- $L_i$  = Initial  $D_1$  length at  $20^\circ C$  (598.229 mm) (nominal module of  $D_1$  measured with the same coordinate measuring machine previously refereed),
- $\Delta T$  = Temperature range considered during measuring ( $\pm 5^\circ C$ ).

Finally, the magnitudes related to environmental conditions,  $X_{18}$ ,  $X_{19}$  and  $X_{20}$  are only mentioned but not quantified because measurements were carried out in an indoor work area, free of sunlight effects. As ARSECOND [6] indicates, the changes considered bring no significant effects on the measurements, as well as in barometric pressure changes. However, due care should be taken as any optical instrument to prevent severe temperature gradients. This gradient effect may be mitigated somewhat by using a greater number of transmitters, but cannot be eliminated.

The Tab. 1 presents all the uncertainty contributions considered in a measurement process with the iGPS and its calculations.

Table 1. Balance of iGPS measurement uncertainties. Source: Landeta [11].

Magnitude		Estimative	Uncertainty contribution		Probability distribution	Sensitivity coefficient	Standard uncertainty	Degrees of Freedom
<b>Transmitters</b>								
X1	Azimuth angle	--	0.50 "	0.017 mm	retangular n = 3	1	0.0098 mm	∞
X2	Elevation angle	--	0.50 "	0.017 mm	retangular n = 3	1	0.0098 mm	∞
X3	Symmetry of the laser beam	--	1 "	0.034 mm	retangular n = 3	1	0.0196 mm	∞
X4	Transmitter average error	--	--	0.122 mm	normal k = 2	1	0.0610 mm	∞
X5	Precession of rotation axis	--	0.50 "	0.017 mm	retangular n = 3	1	0.0098 mm	∞
X6	Noise in spin-axis bearings	--	0.50 "	0.017 mm	retangular n = 3	1	0.0098 mm	∞
<b>Sensors</b>								
X7	Geometry / mini-bar vector material	--	--	--	--	--	--	--
X8	Geometry of sensors side surfaces	--	--	0.030 mm	retangular n = 3	1	0.0173 mm	∞
X9	Pulse distortion of amplifier	--	2.50 "	0.085 mm	retangular n = 3	1	0.0491 mm	∞
X10	Analog to digital conversion error	--	0.82 "	0.028 mm	retangular n = 3	1	0.0162 mm	∞
X11	Virtual frame error of reference system	--	--	0.037 mm	normal k = 2	1	0.0185 mm	∞
X12	Mini-vector bar frame error	--	--	0.132 mm	normal k = 2	1	0.0660 mm	∞
X13	iProbe calibration	--	--	--	--	--	--	--
X14	Laser beam reflection ( $D_l$ )	598.229 mm	--	0.445 mm	retangular n = 3	0.0002	0.0001 mm	∞
<b>Scale bar</b>								
X15	Geometry / material of the scale bar	--	--	--	--	--	--	--
<b>Sample test</b>								
X16	Standard deviation of distance $D_l$ with iGPS	598.207 mm	--	0.012 mm	normal n = 3	1	0.0069 mm	2
X17	Geometry / material of sample test	598.229 mm	--	0.036 mm	retangular n = 3	1	0.0207 mm	∞
<b>Environmental conditions</b>								
X18	Temperature / moisture	--	--	--	--	--	--	--
X19	Vibrations and air flows	--	--	--	--	--	--	--
X20	Brightness / reflective surfaces	--	--	--	--	--	--	--
							<b>Effective degrees of freedom</b>	<b>138622</b>
							<b>Combined standard uncertainty</b>	<b>0.112 mm</b>
							<b>Coverage factor - k</b>	<b>2.00</b>
							<b>Expanded measurement uncertainty</b>	<b>0.23 mm</b>

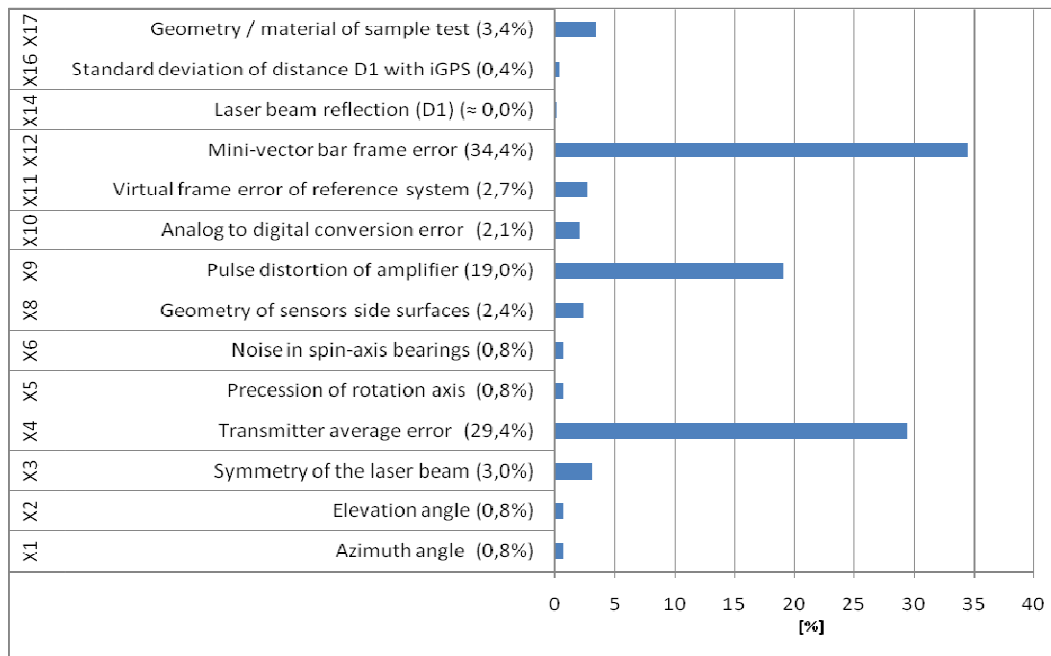


Fig. 9. Contribution of the uncertainties percentage iGPS for measuring distance. Source: Landeta [11].

### 3.4 Uncertainties analysis

The percentage contribution of each one of the uncertainty sources of the Tab. 1 is showed in the Fig. 9. Where, it can be observed that the three largest sources of uncertainty contribution equal 82.8% of the total amount of iGPS uncertainty measurements. These sources are the transmitter average error ( $X_4$ ), the pulse distortion of amplifier ( $X_9$ ) and the mini-vector bar frame error ( $X_{12}$ ).

Regarding to the error of amplifier distortion pulse under the work area conditions where the experiments were carried out, their uncertainty contribution cannot be less than 0.085 mm. Because, as is indicated by ARSECOND [6], an angular error of 2.5" corresponds to the linear uncertainty said, and it is caused when the distance between transmitters and sensors is in the range up to 10 m. But for longer distances, the angular error is reduced to 0.5", reducing the uncertainty contribution 0.017 mm.

In the work volume calibration (transmitters positioning), The use of the iGPS scale bar influences directly on transmitter average error ( $X_4$ ) and mini- vector bar error ( $X_{12}$ ). Considering the iGPS manufacturer guidelines [9], the mini-vector bar frame error ( $X_{12} = 0.132$  mm) is in the range of 0.102 mm to 0.203 mm. The system accuracy level in this range is seen as very good. While the transmitter average error ( $X_4 = 0.122$  mm) is in another range of values lower than 0.152 mm with an excellent qualification of its system accuracy level. Thereby, these uncertainty contributions meet the requirements suggested by the iGPS system manual [9].

In order to understand the system behavior related to mini-vector bar and iProbe uncertainties it is carried out the same procedure described above, determining the transmitter average error ( $X_4$ ) and the virtual frame error of reference system ( $X_{11}$ ) that is represented in the Tab 2. The error of the local coordinate system, now using the iProbe ( $X_{12}$ ), the measurements standard deviation ( $X_{16}$ ) and other angular uncertainty contributions in terms of distances (transmitter - sensor) can be combined and summarized in the Tab. 3 in the form of expanded uncertainties.

**Table 2. Transmitter average error ( $X_4$ ) and error of the local coordinate system ( $X_{11}$ ) (Used for mini-vector bar and iProbe.) Source: Landeta [11].**

Transmitter quantity	$X_4$	$X_{11}$	$X_4$	$X_{11}$	$X_4$	$X_{11}$	$X_4$	$X_{11}$	$X_4$	$X_{11}$
	[mm]	[mm]	[mm]	[mm]	[mm]	[mm]	[mm]	[mm]	[mm]	[mm]
2	0,046	0,184	0,041	0,086	0,036	0,082	0,044	0,084	0,036	0,043
3	0,089	0,123	0,084	0,034	0,072	0,036	0,077	0,040	0,062	0,039
4	0,086	0,104	0,095	0,075	0,086	0,079	0,091	0,060	0,086	0,024
5	0,112	0,056	0,114	0,045	0,101	0,043	0,118	0,026	0,104	0,014
6	0,065	0,054	0,111	0,024	0,123	0,012	0,119	0,019	0,122	0,037
	3 m		4 m		5 m		6 m		7 m	
	Transmitter - sensor distance (d)									

Table 2 shows an estimation of expanded uncertainties of iGPS measurements depending on the type of sensor, quantity of transmitters and distances of the measuring point.

**Table 3. iGPS system uncertainty in terms of sensor type, transmitter quantity and distances from the measurement point. Source: Landeta [11].**

EXPANDED UNCERTAINTY OF MEASUREMENT [mm]										
Transmitter quantity	iProbe	Mini vector bar	iProbe	Mini vector bar	iProbe	Mini vector bar	iProbe	Mini vector bar	iProbe	Mini vector bar
	2	±0,84	±0,21	±0,82	±0,15	±0,77	±0,15	±0,85	±0,18	±0,89
3	±0,87	±0,23	±0,83	±0,19	±0,84	±0,19	±0,86	±0,18	±0,77	±0,23
4	±0,80	±0,23	±0,81	±0,22	±0,80	±0,22	±0,84	±0,20	±0,66	±0,21
5	±0,84	±0,21	±0,84	±0,20	±0,86	±0,19	±0,85	±0,22	±0,86	±0,20
6	±0,85	±0,23	±0,88	±0,19	±0,86	±0,21	±0,87	±0,20	±0,89	±0,23
	3 m		4 m		5 m		6 m		7 m	
	Distance d between transmitter and sensor									

### 4. CONCLUSION

Considering the mini-vector bar, the iGPS system uncertainty is around  $\pm 0.23$  mm, regardless of the transmitter quantity at distances from 3 m to 7 m. Thus, it can be concluded that these results validate the technical information of the iGPS manufacturer datasheet ( $\pm 0.25$  mm) [9].

On the other hand, with respect to iProbe, the iGPS system uncertainty is around  $\pm 0.90$  mm, regardless of the transmitters quantity within distances evaluated, against the technical information of manufacturer's manual. It can be observed that the main cause is the error of its own frame generated by the iProbe, being always higher than the frame generated by the vector mini-bar. The iProbe frame error (average 0.821 mm) is always presented more than four times the mini-vector bar frame error (0.125 mm).

It should be remembered that this process is to measure the distance D1 (distance between the mini-vector bar and the origin of the reference frame) with the vector mini-bar, at an average distance of 7 m from each of the 06 active transmitters at the sensors.

### ACKNOWLEDGMENTS

The authors acknowledge financial support from the Brazilian government agencies: FAPESP, CNPq, CAPES and FINEP.

### REFERENCES

- [1] Y. Hada, et al, "Trajectory Tracking Control of a Non-Holonomic Mobile Robot using Igps and Odometry", In: IEE, New York.USA, 2003.
- [2] C. Depenthal, J. Schwendemann, "IGPS – A New System for Static and Kinematic Measurements", Optical 3-D Measurement Techniques IX, 2009.
- [3] W. Cuypers, et al, "Optical measurement techniques for mobile and large-scale dimensional metrology", ELSEVIER, 2009.
- [4] P. G. Maropoulos, et al, "Large Volume Metrology Process Models: a Framework for Integrating Measurement with Assembly Planning", ELSEVIER, 2008.

- [5] J. E. Muelaner, et al, “*Study of the Uncertainty of Angle Measurement for a Rotary-Laser Automatic Theodolite (R-LAT)*”, ImechE, v. 223, part b, p. 217-229, 2009.
- [6] ARC SECOND, “*Constellation 3Di: Error Budget and Specifications.*”, Dulles, 2002.
- [7] ARC SECOND, “*GPS Indoor: Work Space: Industrial Measurement Edition: User’s Guide, version 6.0*”, Dulles, 2005.
- [8] B. Landeta, R. Sutério “*Study of the influence of distance and transmitters number in coordinate measuring using the iGPS system - indoor global positioning system*”, 6th National Congress of Mechanical Engineering, Campina Grande, Brasil.
- [9] METRIS, “*Ispace, Ontario, Canada. Portable Metrology Systems User Manual and Startup Guide*”, 2009.
- [10] D. A. Maisano, et al “*Indoor GPS: system functionality and initial performance evaluation*”, International Journal of Manufacturing Research, v. 3, n. 3, pp. 335-349, 2008.
- [11] B. Landeta, “*Evaluation of the Metrological Performance of the iGPS Measurement System*”, Master thesis (in portuguese), Technological Institute of Aeronautics ITA, São José dos Campos, Brazil. 2010.
- [12] INMETRO, “*International Vocabulary of Basic and General Terms in Metrology*”, 2005,
- [13] INMETRO, “*International Vocabulary of Basic and General Terms in Metrology*”, 2005, “*Guide to expression of measurement uncertainty*”, 2003.
- [14] INTERNATIONAL STANDARDIZATION ORGANIZATION. ISO/DTS 15330-3, “*E. geometrical product specifications (Gps): coordinate measuring machines (CMM): techniques for determining the uncertainty of measurement - part 3: uncertainty assessment using calibrated workpieces*”, Geneva, 2000.